THE JOURNAL OF BIOLOGICAL CHEMISTRY VOL. 288, NO. 20, pp. 14463–14475, May 17, 2013

Metabolomic Profiling Reveals a Role for Caspase-2 in Lipoapoptosis*

Received for publication, November 26, 2012, and in revised form, April 2, 2013 Published, JBC Papers in Press, April 3, 2013, DOI 10.1074/jbc.M112.437210

Erika Segear Johnson[‡1], Kelly R. Lindblom[‡1], Alexander Robeson[‡], Robert D. Stevens[§¶], Olga R. Ilkayeva[§], Christopher B. Newgard[‡§], Sally Kornbluth[‡2], and Joshua L. Andersen[¶3]

From the Departments of [‡]Pharmacology and Cancer Biology and [¶]Medicine, Duke University Medical Center, Durham, North Carolina 27708 and [§]Sarah W. Stedman Nutrition and Metabolism Center, Duke University Medical Center, Durham, North Carolina 27704

Background: Prior experiments described the metabolic regulation of caspase-2, but the underlying caspase-2-activating stimulus was unknown.
Results: Metabolomics implicated an accumulation of long-chain fatty acid (LCFA) metabolites in caspase-2 activation.
Conclusion: Caspase-2 is activated by an overabundance of saturated LCFAs and is required for cell death.
Significance: These findings provide mechanistic insight into LCFA-induced apoptosis, highlighting a novel role for caspase-2 in this setting.

The accumulation of long-chain fatty acids (LCFAs) in non-adipose tissues results in lipid-induced cytotoxicity (or lipoapoptosis). Lipoapoptosis has been proposed to play an important role in the pathogenesis of several metabolic diseases, including non-alcoholic fatty liver disease, diabetes mellitus, and cardiovascular disease. In this report, we demonstrate a novel role for caspase-2 as an initiator of lipoapoptosis. Using a metabolomics approach, we discovered that the activation of caspase-2, the initiator of apoptosis in *Xenopus* egg extracts, is associated with an accumulation of LCFA metabolites. Metabolic treatments that blocked the buildup of LCFAs potently inhibited caspase-2 activation, whereas adding back an LCFA in this scenario restored caspase activation. Extending these findings to mammalian cells, we show that caspase-2 was engaged and activated in response to treatment with the saturated LCFA palmitate. Down-regulation of caspase-2 significantly impaired cell death induced by saturated LCFAs, suggesting that caspase-2 plays a pivotal role in lipid-induced cytotoxicity. Together, these findings reveal a previously unknown role for caspase-2 as an initiator caspase in lipoapoptosis and suggest that caspase-2 may be an attractive therapeutic target for inhibiting pathological lipid-induced apoptosis.

During periods of overnutrition, LCFAs[4] accumulate to levels that exceed the storage capacity of adipose tissue. As a result, LCFAs become elevated in the plasma, resulting in increased import and storage of these molecules in non-adipose tissues (1–3). The overaccumulation of lipids in non-adipose tissues can be toxic, resulting in chronic cellular dysfunction and ultimately apoptotic cell death, a process more generally referred to as lipoapoptosis. Lipoapoptosis can profoundly compromise tissue function and appears to be an underlying cause of diseases associated with metabolic syndrome (3–6).

LCFA-induced lipoapoptosis has been shown to occur in many cell types, including hepatocytes, cardiomyocytes, proximal tubule cells in the kidney, and islet beta cells in the pancreas (7–10). These cells, which specifically undergo apoptosis in response to treatment with saturated fatty acids, display several characteristic features of the intrinsic apoptotic pathway, including mitochondrial permeabilization, cytochrome *c* release, and effector caspase activation (11). Activation of this pathway is regulated by members of the Bcl-2 family of proteins, whereby proapoptotic BH3-only proteins (*i.e.* Bid, Bad, etc.) sequester antiapoptotic Bcl-2 proteins (*i.e.* B cell lymphoma X_L (Bcl-xL)) away from Bax/Bak, allowing them to oligomerize and induce mitochondrial outer membrane permeabilization and release of cytochrome *c* (12). Once cytosolic, cytochrome *c* forms a multimeric complex with the apoptotic protease-activating factor Apaf-1, resulting in recruitment and activation of caspase-9. This complex, termed the apoptosome, cleaves and activates the executioner caspases, caspase-3 and -7, which then dismantle the cell (13, 14). Although the role of the intrinsic apoptotic pathway has been well established in LCFA-induced apoptosis, the core apoptotic machinery engaged by toxic concentrations of saturated LCFAs upstream of the mitochondria has not been revealed.

Despite being one of the most conserved caspases, the regulation and precise functions of caspase-2 have remained somewhat unclear. In certain settings (*e.g.* heat shock, microtubule-targeted chemotherapeutics, and pore-forming toxins), caspase-2 has been shown to function as an initiator caspase that works upstream of the mitochondria to promote cytochrome *c* release (15–17). The prevailing model is that

* This work was supported, in whole or in part, by National Institutes of Health Grants GM080333 (to S. K.) and 5F31CA165545-02, a Ruth L. Kirschstein National Research Service Award (to E. S. J.).
[1] Both authors contributed equally to this work.
[2] To whom correspondence may be addressed: Dept. of Pharmacology and Cancer Biology, Duke University Medical Center, P. O. Box 3813, C370 LSRC Research Dr., Durham, NC 27710. Tel.: 919-613-8624; Fax: 919-681-1005; E-mail: kornb001@mc.duke.edu.
[3] To whom correspondence may be addressed: Dept. of Chemistry and Biochemistry, Brigham Young University, E111 BNSN, 685 E. University Pkwy., Provo, UT 84602. Tel.: 801-422-7193; Fax: 801-422-0163; E-mail: jandersen@chem.byu.edu.
[4] The abbreviations used are: LCFA, long-chain fatty acid; TCA, tricarboxylic acid; AOA, aminooxyacetate; Bcl-xL, B cell lymphoma X_L; NAFLD, nonalcoholic fatty liver disease; *p*NA, *p*-nitroanaline.

caspase-2 once activated cleaves the BH3-only protein Bid to generate truncated Bid, which activates Bax to promote cytochrome *c* release (18, 19).

Physiologically, the role of caspase-2 is not entirely clear. The only overt developmental phenotype in the caspase-2 KO mouse was an overabundance of oocytes, suggesting a central role for caspase-2 in controlling oocyte death (20). Our laboratory has used *Xenopus laevis* oocytes and eggs to study the metabolic regulation and activation of caspase-2 (21–23). We demonstrated previously that the prolonged incubation of egg extract at room temperature leads to activation of the apoptotic cascade via caspase-2 and that caspase-2 is required for apoptosis in this system (21). Moreover, we found that caspase-2 activation in the extract occurred only after specific metabolic changes (*e.g.* depletion of NADPH and NAD^+) and more importantly could be suppressed by supplementing the extract with metabolites expected to lead to NADPH production either through malic enzyme or the pentose phosphate pathway (21, 22). Based in part on these observations, we suspected that the spontaneous activation of caspase-2 occurs in response to a progressive metabolic stress or depletion of specific metabolites.

In an attempt to more thoroughly understand the metabolic changes that underlie caspase-2 activation, we performed metabolomic profiling on the egg extract at time points leading up to caspase-2 activation. Consistent with previous studies on egg metabolism, we observed a robust decrease in aspartate upon extract incubation, indicating the usage of amino acids as a fuel source in this cell type (24, 25). The most notable change preceding caspase-2 activation, however, was a marked increase in LCFA metabolites. We show here that metabolic treatments that suppressed caspase-2 activation specifically blocked this increase in LCFA metabolites, suggesting that a buildup of lipids may engage the apoptotic pathway/caspase-2 in egg extract. Moreover, the caspase-suppressive effect of such metabolic treatments could be overridden by supplementing the extract with the saturated LCFA palmitate. Extending this finding, we demonstrate that caspase-2 was activated by recruitment to a high molecular weight complex in mammalian cells following palmitate treatment. Caspase-2 activity was significantly increased following palmitate treatment, and downregulation of caspase-2 significantly impaired cell death induced by saturated LCFAs, revealing a conserved, critical role for caspase-2 in mediating LCFA-induced lipoapoptosis. These findings may have clinical implications for the treatment of diseases associated with lipid accumulations.

EXPERIMENTAL PROCEDURES

Preparation of Xenopus Egg Extracts and Metabolomic Profiling—Xenopus egg extracts were prepared according to the protocol described previously by Smyth and Newport (26). Freshly prepared *Xenopus* egg extracts (300 μl) or extracts incubated at room temperature for 3–4 h (300 μl) were used for metabolic profiling. Proteins were first removed by precipitation with methanol (1200 μl) or acidified acetonitrile (750 μl of acetonitrile + 450 μl of 1% formic acid). Samples were mixed well by vortexing and spun down, and supernatants were removed immediately for amino acid, organic acid, and acylcarnitine analysis. Measurements of amino acid and acylcarnitine were made by flow injection electrospray tandem mass spectrometry of their butyl and methyl esters, respectively (27), using a Waters Acquity^{TM} UPLC system equipped with a triple quadrupole detector and a data system controlled by MassLynx 4.1 operating system (Waters, Milford, MA). For organic acid, analytes were extracted into ethyl acetate, dried, and then converted to trimethylsilyl esters by *N*,*O*-bis(trimethylsilyl)trifluoroacetamide with protection of α-keto groups by oximation with ethoxyamine hydrochloride. Organic acids were analyzed by capillary gas chromatography/mass spectrometry (GC/MS) using a TRACE DSQ instrument (Thermo Electron Corp., Austin, TX). All MS analyses used stable isotope dilution with internal standards from Isotec (St. Louis, MO), Cambridge Isotope Laboratories (Andover, MA), and CDN Isotopes (Pointe-Claire, Quebec, Canada). NADH levels were measured using an NAD^+/NADH quantitation kit (BioVision, Mountain View, CA). Oxygen (O_2) consumption rates were measured using the Seahorse extracellular flux XF24 analyzer (Seahorse Biosciences, North Billerica, MA). Briefly, freshly prepared egg extracts were added in triplicate to a 24-well plate and analyzed for 4 h. O_2 consumption rates were assessed using the "(Level) Direct (Ksv)" method.

Caspase Activity Assays—For egg extract experiments, caspase-3 activity was measured spectrophotometrically by assessing the cleavage of the colorimetric substrate Ac-DEVD-*p*NA. Briefly, 5-μl aliquots of extract were removed, transferred to 85 μl of DEVDase buffer (50 mM HEPES (pH 7.5), 100 mM NaCl, 0.1% CHAPS, 10 mM DTT, 1 mM EDTA, and 10% glycerol), and kept on ice. Following collection of all samples, 10 μl of Ac-DEVD-*p*NA (200 μm) was added to each sample and incubated at 37 °C for 30–60 min. Absorbance was measured at 405 nm. Caspase-2 activity assays were performed according to the BioVision caspase-2 colorimetric assay kit specifications. Briefly, for extract experiments, 10-μl aliquots of extract were transferred to 40 μl of cell lysis buffer and diluted with 50 μl of 2× reaction buffer and 10 μl of VDVAD-*p*NA (4 mM) at 37 °C for 60–120 min. Absorbance was measured at 405 nm.

Analysis of Protein Processing—^{35}S-Labeled caspase-2 proteins were synthesized using the TnT SP6 quick coupled transcription/translation system (Promega, Madison, WI). Briefly, 20 ng/ml pSP64T caspase-2 cDNA was added to rabbit reticulocyte lysate containing 0.4 mCi/ml ^{35}S Translabel along with additional components in accordance with the manufacturer's protocol. Radiolabeled proteins were added to the extract, and proenzyme processing was assayed by SDS-PAGE followed by PhosphorImager detection (GE Healthcare).

Cell Culture, siRNA, and Palmitate Treatments—All cell lines were grown in DMEM with 10% fetal bovine serum with the exception of the AML12 cells, which were cultured according to ATCC specifications. Custom caspase-2 oligos targeting to the 3′-untranslated region of caspase-2 were ordered from Sigma-Aldrich. The sequence for the caspase-2 siRNA used was UGGAAGUAUUUGAGAGAGA[dT][dT] (square brackets represent nucleotide overhang). SMARTpool mouse caspase-2 siRNA was obtained from Dharmacon (catalogue number M-044184-00), and ON-TARGETplus Control siRNA 1 was obtained from Dharmacon (catalogue number

D-001810-01-05). RNAi reagents were transfected with RNAiMAX (Invitrogen) following the manufacturer's protocol. To avoid the addition of organic solvents to the cell culture medium, solutions containing fatty acid sodium salts bound to albumin were prepared from stock solutions of the fatty acid sodium salt (100 mM) and fatty acid-free BSA (2%). For example, 28 mg of sodium palmitate was dissolved in 1 ml of sterile H_2O at 70 °C, and this solution was added to cell culture medium containing 2% fatty acid-free BSA. These solutions were used after filtration through 0.22-μm filters. Caspase-2 activity assays were performed according to the BioVision caspase-2 colorimetric assay kit specifications. For flow cytometric analysis of cell death, cells were collected, resuspended in 1 μg/ml propidium iodide (dissolved in PBS), and kept on ice until analysis.

Gel Filtration Analysis—293T cells were treated with 2% BSA or 2% BSA + 1 mM palmitate for 18 h before lysis by Dounce homogenization in hypotonic lysis buffer (20 mM HEPES (pH 7.5), 10 mM KCl, 1.5 mM $MgCl_2$, 1 mM EDTA, 1 mM EGTA, 1 mM DTT, and 5 μg/ml each aprotinin and leupeptin). Lysates were centrifuged at 4 °C for 15 min at 13.2 rpm, and protein concentration of the supernatant was determined using the Bio-Rad protein assay reagent. 500 μl of 8 mg/ml lysates was loaded onto a Superdex 200 column at a flow rate of 0.3 ml/min to collect fractions.

Antibodies and Additional Reagents—Anti-caspase-2 (polyclonal; 1:1000) was purchased from Abcam (ab7979); anti-caspase-2 (monoclonal; 1:1000) was from BD Transduction Laboratories (Clone G310–1248), and anti-actin (polyclonal; 1:1000) was from Santa Cruz Biotechnology (I-19). Aminooxyacetate (Sigma-Aldrich) was used at 10 mM. D-Glucose 6-phosphate sodium salt (Sigma-Aldrich) was used at 20 mM. Triacsin C, etomoxir, and fatty acid sodium salts were purchased from Sigma-Aldrich with the exception of sodium palmitoleate, which was purchased from Nu-Chek Prep, Inc. Bovine serum albumin (Fraction V; heat shock; fatty acid ultra-free) was purchased from Roche Applied Science.

RESULTS

Amino Acid Metabolism and the Accumulation of Succinate and Long-chain Acylcarnitines Precede Caspase Activation in Xenopus Egg Extract—Active caspase-2 has been shown to trigger mitochondrial cytochrome *c* release in a number of settings, and we have shown that it is required upstream of mitochondria to induce cell-free apoptosis in the *Xenopus* egg extract system (21). We initially observed that activation of caspase-2 in this setting could be blocked by supplementing egg extract with metabolic intermediates, suggesting that metabolic changes preceded caspase-2 activation. However, the precise nature of these metabolic changes was unclear. Thus, in an effort to understand the mechanisms underlying caspase-2 activation, we performed metabolomics on *Xenopus* egg extract, comparing fresh, unaged extract with extract incubated at room temperature for several hours and harvested just prior to caspase-2 activation (aged). All samples were analyzed for amino acid, organic acid, and acylcarnitine changes.

In agreement with previous studies on egg metabolism, the two most abundant amino acids in *Xenopus* egg extract were aspartate and glutamate (28, 29). Interestingly, upon room temperature incubation of the extract, we observed a notable decrease in aspartate along with a corresponding increase in alanine with very little change in the other amino acids profiled (Fig. 1*A*). These changes are likely occurring via transamination reactions whereby aspartate is converted to oxaloacetate and pyruvate is converted to alanine via transamination of α-ketoglutarate and glutamate, respectively (Fig. 1*B*). The decrease in aspartate suggests that this amino acid is likely serving as a carbon source to support extract metabolism as has been shown previously in intact *Xenopus* eggs (24). We also observed changes in the organic acid profile of fresh and aged extracts, including an increase in both pyruvate and lactate following extract incubation (Fig. 1*C*). In contrast, intermediates of the tricarboxylic acid (TCA) cycle decreased moderately with the exception of succinate, which showed significant accumulation (Fig. 1*C*).

Increased levels of succinate are often observed under conditions in which the electron transport chain is inhibited (30–32). Hypoxia (or the lack of oxygen) has been shown to inhibit electron transport chain function as well as result in increased levels of succinate. Interestingly, under hypoxic conditions, the formation of succinate has been shown to be coupled to amino acid utilization, specifically that of aspartate and glutamate (33, 34). Given the similarities between these observations and our data, we wanted to determine whether there were any other metabolic changes that might indicate a loss of mitochondrial respiration. Because electron transport chain inhibition results in a block in β-oxidation and a decrease in the NAD^+/NADH ratio, we examined both the lipid profile and redox status of incubated extract. Consistent with a lack of electron transport chain function, we observed an accumulation of multiple long-chain acylcarnitines reflective of the long-chain acyl-CoA pools as well as a progressive decrease in the NAD^+/NADH ratio following extract incubation (Fig. 1, *D* and *E*). Furthermore, because changes in the cytosolic levels of NADH and NAD^+ are reflected in the balance between lactate and pyruvate, we assessed the lactate/pyruvate ratio and found that the ratio was significantly increased from 17.3 to 188.7 in aged extracts, supporting the observed accumulation of NADH. Given these data, we wanted to more directly assess whether the extract might be experiencing hypoxia. Rather than assessing the dissolved oxygen content in the extract as a readout of hypoxia as it would be hard to define what dissolved oxygen percentage in egg extracts would result in hypoxic phenotypes, we chose to more directly assess mitochondrial respiration. Using the Seahorse Bioscience XF24 extracellular flux analyzer, we monitored the O_2 consumption rate of aging egg extracts for 4 h. Indeed, extracts showed little O_2 consumption with respiration virtually going to zero over time (Fig. 1*F*). Together, these data suggest that the observed metabolic changes are linked to inhibited mitochondrial respiration, including the formation of succinate from the amino acid aspartate, the buildup of NADH, and the accumulation of LCFA metabolites (acylcarnitines/acyl-CoAs). Because we knew from previous studies that the activation of caspase-2 and downstream apoptotic events could be blocked in this system by supplementing the extract with metabolic

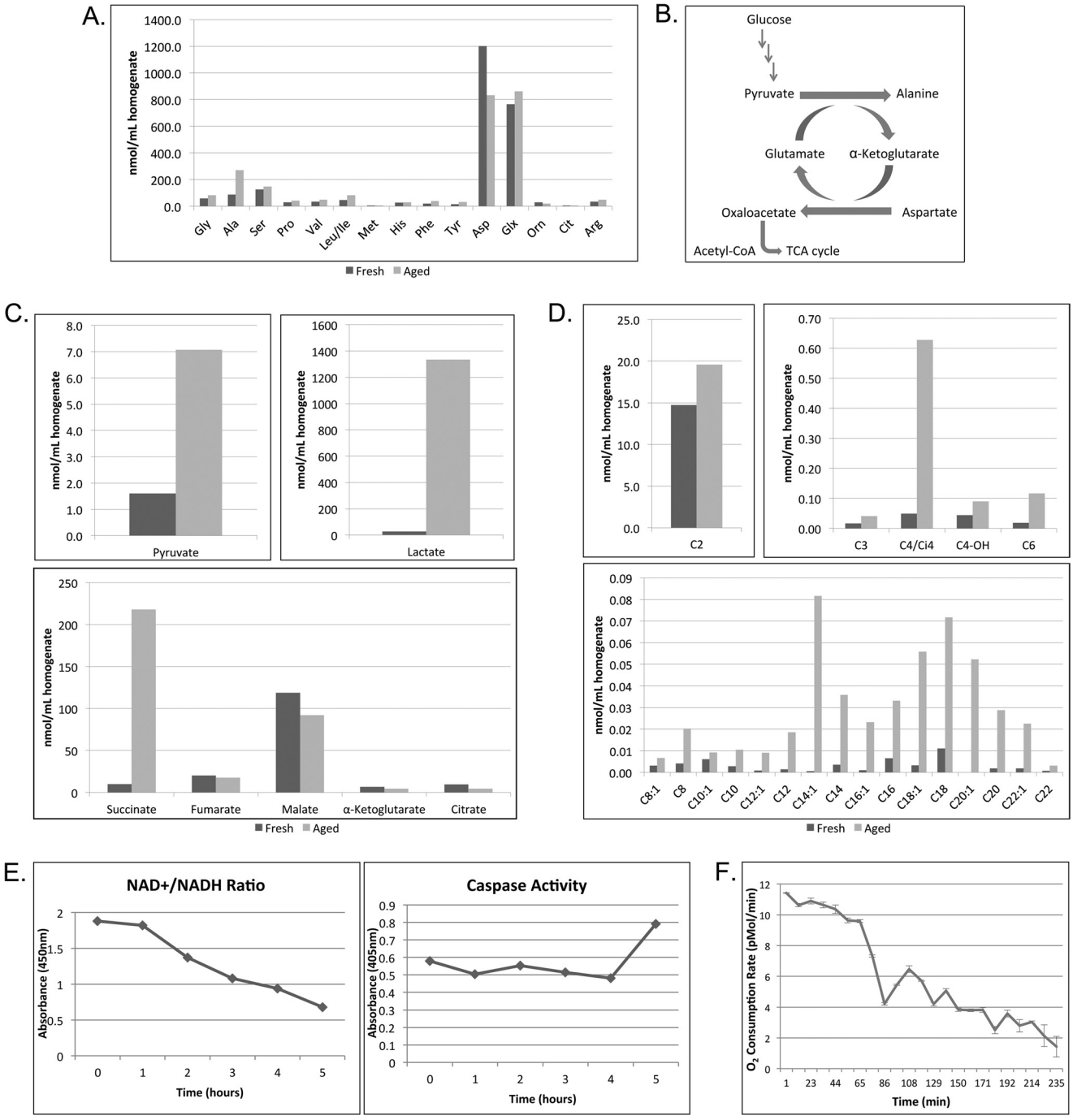

FIGURE 1. **Amino acid metabolism and the accumulation of succinate and long-chain fatty acid metabolites precede caspase activation in *Xenopus* egg extract.** *A*, freshly prepared *Xenopus* egg extract (*Fresh*) or extract incubated at room temperature for 4 h (*Aged*) was analyzed for amino acid profile following protein precipitation. *B*, figure of carbon flux via transamination reactions in the egg extract. *C*, egg extracts treated as in *A* were analyzed for organic acids. *D*, egg extracts treated as in *A* were analyzed for acylcarnitines. *E*, samples of egg extract were collected at the indicated times and analyzed for NAD^+/NADH ratio changes by spectrophotometric color change (kit supplied by BioVision). The same samples were used to measure caspase-3 activity using the caspase substrate Ac-DEVD-*p*NA. Substrate cleavage was measured spectrophotometrically at 405 nm. *F*, the O_2 consumption rate of aging egg extracts was monitored for 4 h using the Seahorse Bioscience XF24 extracellular flux analyzer. The results represent the means ± S.D. (*error bars*) of three technical replicates. *Orn*, ornithine; *Glx*, *glutamine/glutamic acid; Cit, citrulline.*

intermediates (21), we postulated that one of these underlying metabolic changes might be triggering caspase-2 activation.

Inhibition of Amino Acid Transamination by Aminooxyacetate Blocks Caspase Activation—Given the potential dependence of the egg extract on amino acid utilization and previous observations that hypoxia-induced succinate formation could be abrogated by inhibiting transamination reactions (34), we wanted to determine whether the inhibition of transaminase activity would affect caspase activation in the extract. To test this, we treated the extract with the general transaminase inhibitor aminooxyacetate (AOA) and monitored caspase-2 activity via cleavage of the model substrate, VDVAD-*p*NA, over time. Surprisingly, the inhibition of transaminase activity suppressed VDVAD cleavage activity in the extract (Fig. 2*A*; note that the

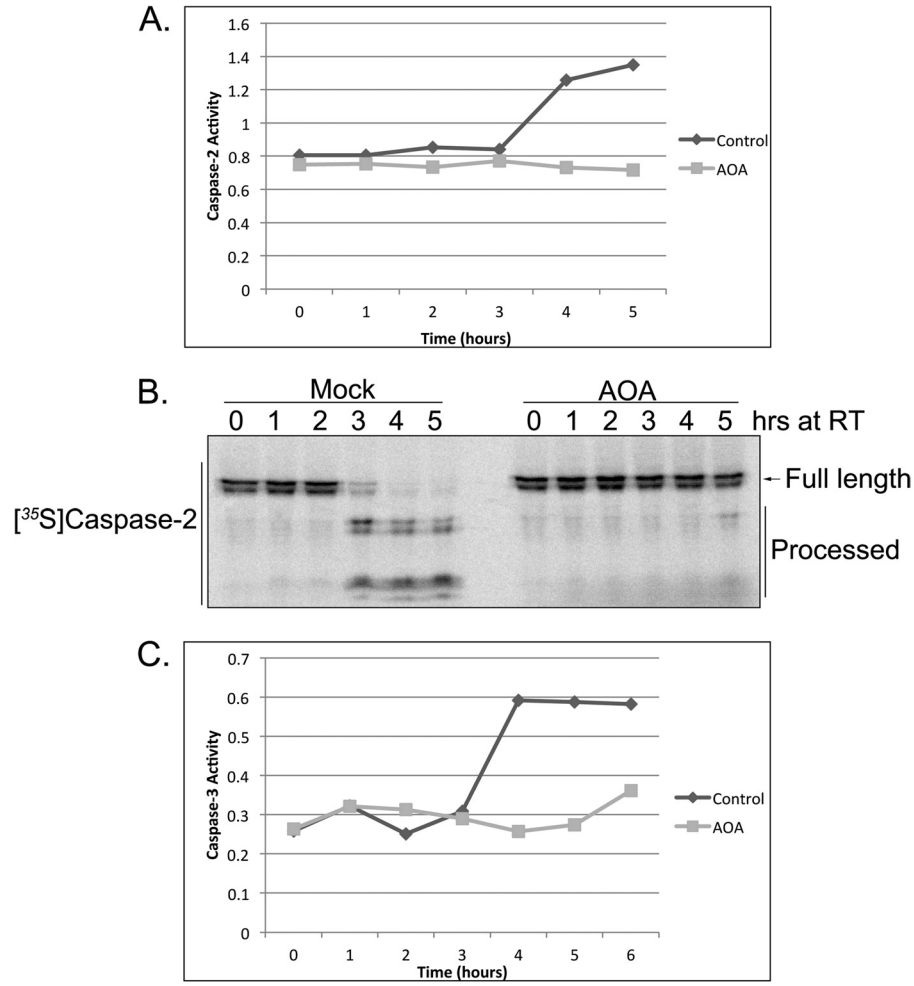

FIGURE 2. **Inhibition of amino acid transamination by AOA blocks caspase activation.** *A*, egg extracts supplemented with AOA (10 mM) or buffer were analyzed for caspase-2 activity at the indicated time points using the BioVision caspase-2 colorimetric assay kit and measuring cleavage of the caspase-2 model substrate, VDVAD-*p*NA, spectrophotometrically. *B*, ^{35}S-labeled caspase-2 was incubated in AOA- or mock-treated extracts, and samples were resolved by SDS-PAGE/PhosphorImager. *C*, egg extracts treated as in *A* were analyzed for caspase-3 activity at the indicated time points using the caspase substrate Ac-DEVD-*p*NA. *RT*, room temperature.

absolute time course of caspase activation varies from extract to extract, but the relative rates of caspase activation following different treatments is constant). We also found that caspase-2 processing, which occurs following caspase-2 activation as a means to stabilize the active dimeric protease, was suppressed by AOA treatment (Fig. 2*B*). Furthermore, downstream activation of the executioner caspase, caspase-3, was also suppressed by AOA treatment (Fig. 2*C*), suggesting that the loss of amino acid transamination can suppress caspase activation in the extract.

Treatment with AOA, which Blocks Caspase Activation, Prevents the Underlying Accumulation of Long Chain Fatty Acid Metabolites—In an effort to understand how inhibition of amino acid transamination can suppress caspase activation, we compared the metabolic profiles of extracts treated with and without AOA. AOA caused aspartate and alanine levels to return to basal levels in aged extracts, consistent with our suggestion that the changes in these amino acids are driven by aspartate transamination and further catabolism (Fig. 3*A*). Treatment of extracts with AOA caused a substantial decrease in TCA cycle intermediates and blocked the accumulation of succinate, suggesting that aspartate plays an important role in energy metabolism, particularly in supplying the extract with anaplerotic substrates (Fig. 3*B*). Glycolytic activity appeared to be unaffected by transaminase inhibition as demonstrated by the accumulation of pyruvate and lactate in the presence of AOA (Fig. 3*B*). Strikingly, we observed a decrease in long-chain acylcarnitine accumulation in the presence of AOA, suggesting that inhibition of amino acid transamination was able to suppress the increase in LCFA metabolites (Fig. 3*C*). Because LCFA accumulation may be linked to redox changes in the extract (*i.e.* high levels of NADH inhibit the oxidation of LCFAs), we assessed whether AOA could modify the observed decrease in the NAD^+/NADH ratio preceding caspase activation. As shown in Fig. 3*D*, AOA was able to delay the decrease in NAD^+/NADH, supporting the notion that acylcarnitine accumulation may be resulting from increasing levels of NADH, which can then feed back to inhibit β-oxidation. Although we observed a delay of NADH accumulation in AOA-treated extracts, the lactate/pyruvate ratio was still increased in comparison with fresh extracts. Although there may be some effect of AOA on cytosolic NAD^+/NADH pools as there was delayed accumula-

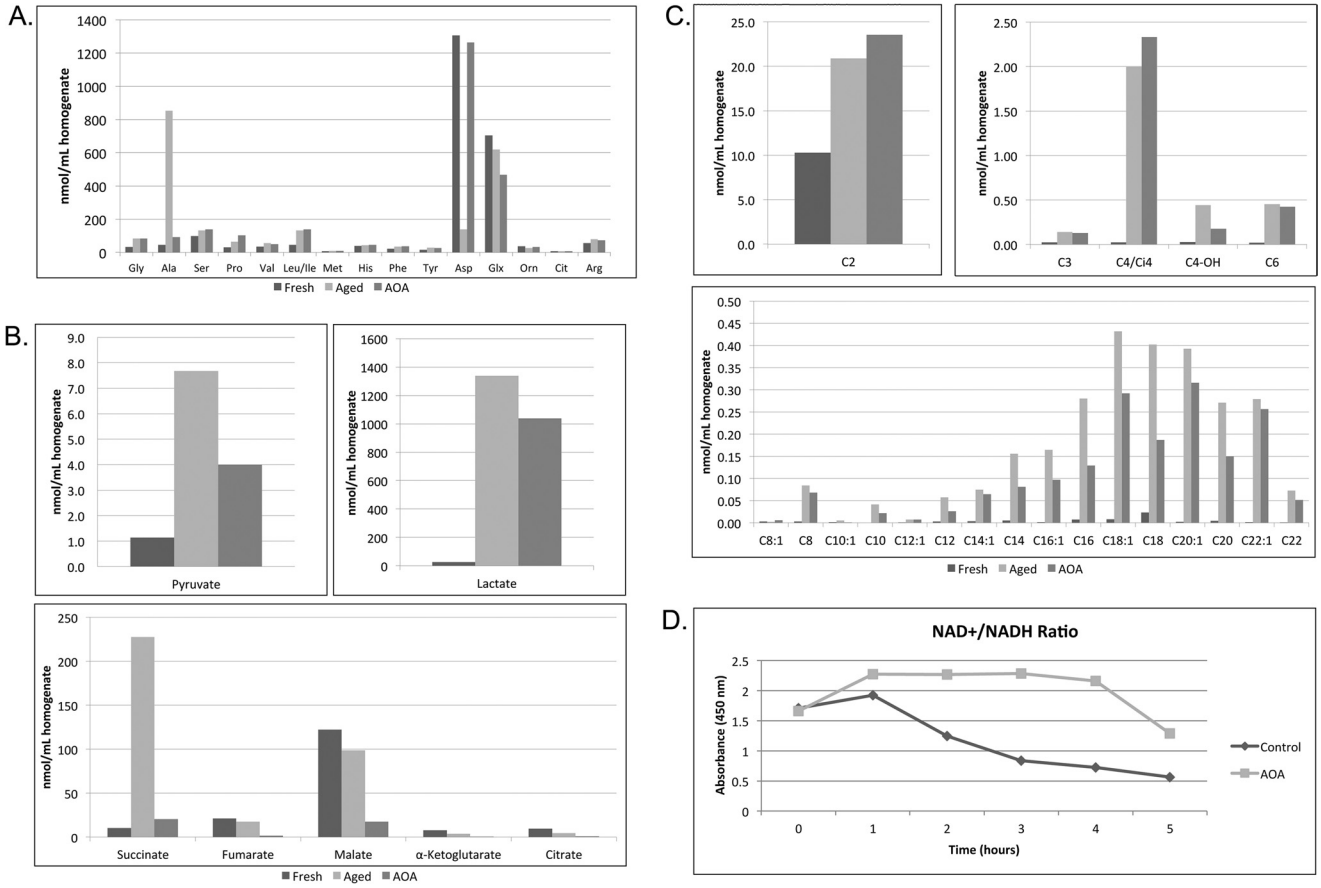

FIGURE 3. **Treatment with AOA, which blocks caspase activation, prevents the underlying accumulation of long chain fatty acid metabolites.** *A*, amino acid profiling was performed on egg extracts immediately following preparation (*Fresh*) or after room temperature incubation in the absence (*Aged*) or presence of 10 mM AOA (*AOA*). *B*, egg extracts treated as in *A* were analyzed for organic acids. *C*, egg extracts treated as in *A* were analyzed for acylcarnitines. *D*, samples of egg extract treated with and without 10 mM AOA were collected at the indicated times and analyzed for NAD^+/NADH ratio changes by spectrophotometric color change (kit supplied by BioVision). *Orn*, ornithine; *Glx, glutamine/glutamic acid; Cit, citrulline.*

tion of lactate (Fig. 3*B*), it is more likely that AOA is blocking the mitochondrial shift of NAD^+ to NADH by inhibiting TCA cycle flux. This in turn may delay the decrease in total NAD^+/NADH.

The ability of AOA to both suppress caspase activation and block significant metabolic changes in the extract, including the catabolism of aspartate and the accumulation of long-chain acylcarnitines, suggests that one or both of these metabolic alterations is necessary for caspase-2 activation (and thus downstream caspase-3 activation) in this system. To further investigate this, we examined the metabolic profile of egg extract treated with a pentose phosphate pathway intermediate, glucose 6-phosphate, which we have previously shown can suppress caspase-2 activation in this setting (21). Although glucose 6-phosphate was able to block the accumulation of long-chain acylcarnitines, it was unable to suppress aspartate transamination and succinate formation (data not shown). Collectively, these data suggest that the accumulation of LCFA metabolites is the pivotal metabolic change underlying caspase-2 activation. Moreover, the previously observed protection from apoptosis in egg extracts conferred by glucose 6-phosphate may be mediated at least in part by preventing the accumulation of LCFAs. These findings raise the interesting possibility that caspase-2 is more broadly an initiator caspase for lipoapoptosis.

Palmitate Accelerates Caspase Activation and Overrides the Protective Effect of AOA—Given the data above and previous publications implicating LCFAs in cell death, we were interested in determining whether treatment of the extract with an LCFA that increased in abundance with extract incubation (palmitate; C16) might accelerate caspase activation (7–10, 35) (Figs. 1*D* and 3*C*). To test this, we treated extracts with BSA-conjugated palmitate or BSA as a control and performed a caspase activity assay. As shown in Fig. 4*A*, palmitate accelerated caspase-3 activation, and this acceleration could be blocked by the addition of the antiapoptotic protein Bcl-xL, suggesting that palmitate is specifically engaging the apoptotic pathway upstream of mitochondria. Furthermore, we verified that the proapoptotic effect of palmitate was being exerted at the level of caspase-2 by monitoring enzyme processing and found that it was indeed accelerated after palmitate treatment (Fig. 4*B*). Together, these data suggest that palmitate can promote caspase-2 activation. Therefore, we reasoned that if AOA was simply blocking the buildup of LCFAs as a means to inhibit apoptosis then palmitate treatment should be able to override the protective effect of AOA. Indeed, palmitate addition was able to overcome the antiapoptotic effect of AOA, accelerating caspase activation (Fig. 4*C*). Taken together, these data suggest that an overabundance of LCFA metabolites can engage the apoptotic pathway in *Xenopus* egg extract where caspase-2 is

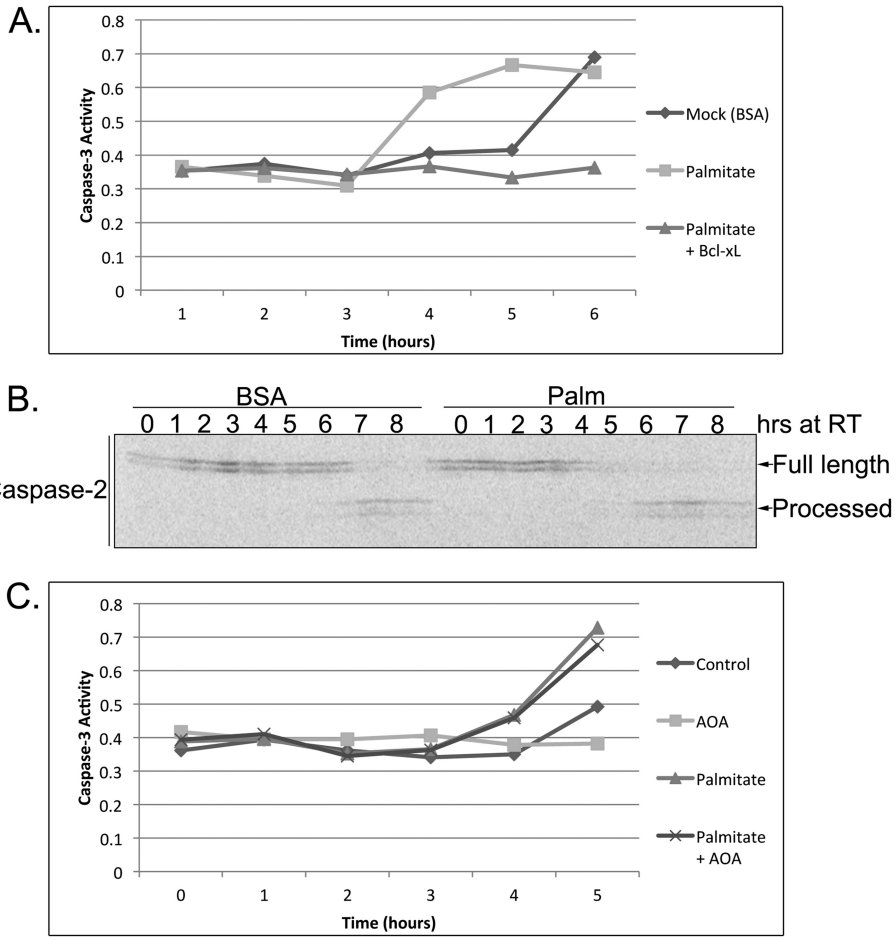

FIGURE 4. **Palmitate accelerates caspase activation and overrides the protective effect of AOA.** *A*, mock-treated (BSA) or palmitate-treated (BSA-conjugated palmitate; 4 mM) egg extracts were incubated in the presence or absence of Bcl-xL and analyzed for caspase-3 activity at the indicated time points. Caspase-3 activity was assessed using the caspase substrate Ac-DEVD-*p*NA, and cleavage was measured spectrophotometrically at 405 nm. *B*, ^{35}S-labeled caspase-2 was incubated in mock- or palmitate (*Palm*)-treated extracts, and samples were resolved by SDS-PAGE/PhosphorImager. *C*, egg extracts were incubated with combinations of palmitate (4 mM) and AOA (10 mM), and caspase-3 activity was assessed using the caspase substrate Ac-DEVD-*p*NA. *RT*, room temperature.

the critical initiator caspase. Importantly, these findings raised the key question as to whether caspase-2 might be a more general initiator of cell death in response to lipotoxicity in mammalian systems.

Caspase-2 Plays a Central Role in Mediating Lipotoxicity in 293T Cells—With ample evidence showing that palmitate can induce cell death in a number of mammalian cell lines at physiologically relevant concentrations (0.03–1.0 mM) (36), we first wished to extend our observations from the *Xenopus* system by determining whether caspase-2 was activated in this cell death process as well. To test this, we transfected HEK 293T cells with siRNA directed against caspase-2 or a scrambled siRNA control and then treated cells with 1 mM palmitate for 18 h. We then assessed caspase-2 activation via cleavage of the model substrate, VDVAD-*p*NA, and found that the enzymatic activity of caspase-2 was increased following palmitate treatment (Fig. 5*A*). The observed increase in activity appears to be specific to caspase-2 as knockdown of the protease was able to block the palmitate-induced increase in substrate cleavage (Fig. 5*A*). Additionally, because caspase-2 has been shown to undergo proteolytic processing following its activation in mammalian cells, we also monitored caspase-2 cleavage via Western blot and found that caspase-2 was processed following palmitate treatment (Fig. 5*B*).

As an initiator caspase, caspase-2 is activated following the binding of adaptor proteins, which facilitate its oligomerization into a high molecular weight complex. Therefore, to determine whether caspase-2 is engaged and activated in this fashion during LCFA-induced apoptosis, we performed gel filtration analysis on HEK 293T cell extracts derived from control and palmitate-treated cells. Although we consistently observed trace amounts of caspase-2 in the high molecular weight fractions of mock-treated cells, palmitate treatment resulted in a robust recruitment of caspase-2 into high molecular weight fractions (Fig. 5*C*). We further confirmed that the caspase-2 present in these high molecular weight fractions was indeed enzymatically active by performing a caspase-2 activity assay (Fig. 5*C*). Together, these data suggest that caspase-2 is activated by recruitment to a high molecular weight complex in mammalian cells following palmitate treatment.

We next wanted to determine whether caspase-2 was required for lipoapoptosis in mammalian cells. To do this, we treated scrambled or caspase-2 knockdown cells with palmitate for 24 h before measuring cell viability. Palmitate induced sig-

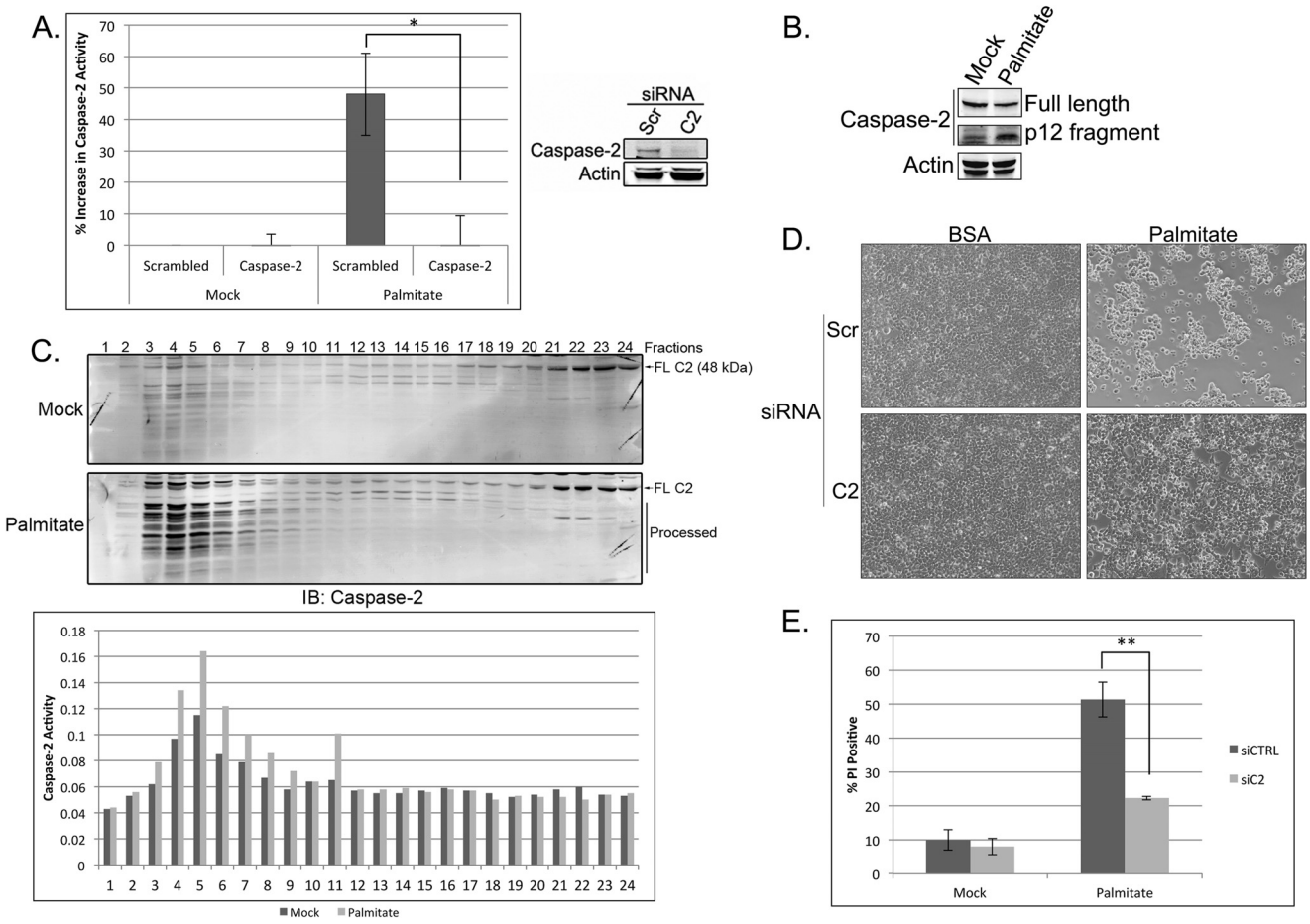

FIGURE 5. **Caspase-2 plays a central role in mediating lipoapoptosis in 293T cells.** *A*, 293T cells were transfected with 50 nM scrambled (*Scr*) or caspase-2 (*C2*)-targeted siRNA. At 48 h post-transfection, cells were mock-treated with BSA or treated with 1 mM palmitate for 18 h, and caspase-2 activity was assessed using the BioVision caspase-2 colorimetric assay kit. Knockdown efficiency was determined by immunoblot. The results represent the means ± S.E. (*error bars*) for percent increase in activity compared with control siRNA-, mock-treated samples for three independent experiments. Statistical significance was determined using a two-tailed Student's *t* test. *, $p < 0.05$ *versus* control. *B*, 293T cells were treated with BSA or palmitate for 24 h and immunoblotted for caspase-2 and actin. The *top* caspase-2 panel is a short exposure (to show changes in full-length caspase-2 levels), and the *bottom* caspase-2 panel is a long exposure (to reveal the p12 fragment). *C*, 293T cells were treated with BSA or palmitate for 18 h before lysis by Dounce homogenization in hypotonic lysis buffer. Cell lysates were separated on a Superdex 200 column, and relevant fractions were immunoblotted (*IB*) for caspase-2. Full-length caspase-2 (*FL C2*) and processed caspase-2 are indicated. Fractions were also tested for caspase-2 activity by assessing cleavage of the caspase-2 model substrate, VDVAD-*p*NA, as part of the BioVision caspase-2 colorimetric assay kit. *D*, 293T cells were treated as in *A*, and at 24 h post-treatment, phase-contrast images were captured on an EVOS FL digital inverted microscope. *E*, 293T cells were treated as in *A*, and cell death was measured 24 h after palmitate treatment by propidium iodide staining and flow cytometric analysis. The results represent the means ± S.E. (*error bars*) for four independent experiments. Statistical significance was determined using a two-tailed Student's *t* test. **, $p < 0.01$ *versus* control. *siCTRL*, control siRNA; *siC2*, caspase-2 siRNA.

nificant cell death in the scrambled control cells, whereas caspase-2-deficient cells were protected from apoptosis as shown by maintenance of cell density over 24 h of treatment (Fig. 5*D*). We further quantified cell death by propidium iodide staining and found that down-regulation of caspase-2 could significantly block palmitate-induced cell death in 293T cells (Fig. 5*E*), suggesting that caspase-2 is required for lipoapoptosis in these cells.

Caspase-2 Mediates Saturated Fatty Acid-induced Lipoapoptosis via Acyl-CoA Cytotoxicity—Previous studies have shown in multiple cell types that only saturated LCFAs exert cytotoxic effects (8, 36–40). Therefore, we wanted to determine whether caspase-2 was required for cell death induced by other saturated LCFAs as well as validate that only saturated LCFAs could induce apoptosis. To do this, we treated scrambled or caspase-2 knockdown cells with monounsaturated fatty acids palmitoleate (16:1) and oleate (18:1) and saturated fatty acids palmitate (16:0) and stearate (18:0) and assessed cell death by propidium iodide staining. As expected, only saturated fatty acids induced prominent cell death (Fig. 6*A*). Interestingly, the loss of caspase-2 was able to significantly protect against cell death induced by both saturated LCFAs, suggesting that caspase-2 can function as a general initiator of cell death in saturated fatty acid-induced lipotoxicity (Fig. 6*A*). Moreover, because the combination of saturated and unsaturated fatty acids has been shown to reduce the cytotoxic effects of saturated fatty acids (41–45), we also assessed whether oleate addition could protect against caspase-2-mediated cell death induced by palmitate or stearate. Consistent with previous findings, oleate was able to block cell death induced by these saturated fatty acids, suggesting that it could prevent palmitate- and stearate-induced caspase-2 activation (Fig. 6*A*).

In some settings, the ability of oleate to suppress the cytotoxic effects of saturated LCFAs has been attributed to its ability

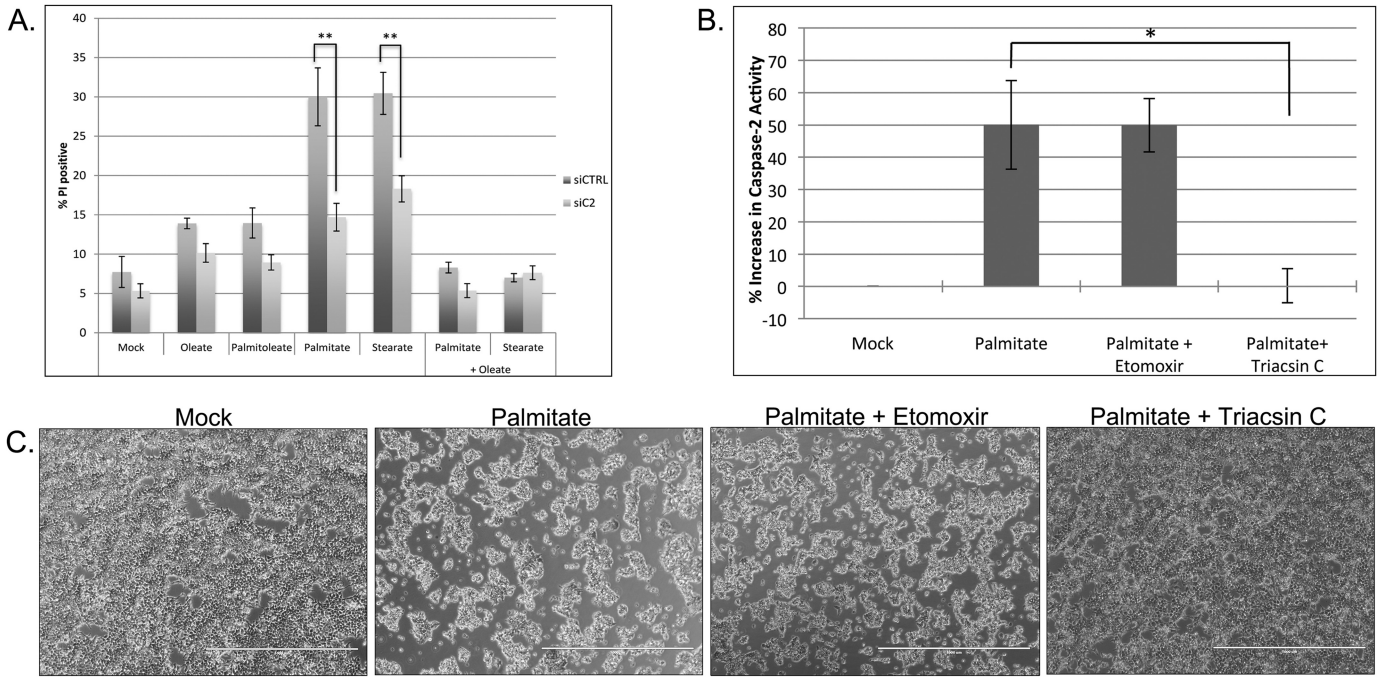

FIGURE 6. **Caspase-2 mediates saturated fatty acid-induced lipoapoptosis via acyl-CoA cytotoxicity.** *A*, 293T cells were transfected with 50 nM scrambled or caspase-2 (*C2*)-targeted siRNA. At 48 h post-transfection, cells were mock-treated with BSA or 1 mM fatty acids, and cell death was measured 24 h post-treatment by propidium iodide (*PI*) staining and flow cytometric analysis. The results represent the means ± S.E. (*error bars*) for four independent experiments. Statistical significance was determined using a two-tailed Student's *t* test. **, $p < 0.01$ *versus* control. *B*, 293T cells were mock-treated with BSA or treated with 1 mM palmitate with or without 200 μM etomoxir or 5 μM triacsin C. At 24 h post-treatment, phase-contrast images were captured on an EVOS FL digital inverted microscope. *C*, 293T cells were treated as in *B*. At 18 h post-treatment, caspase-2 activity was assessed using the BioVision caspase-2 colorimetric assay kit. The results represent the means ± S.E. (*error bars*) for percent increase in activity compared with mock-treated samples for four independent experiments. Statistical significance was determined using a two-tailed Student's *t* test. *, $p < 0.05$ *versus* control. *siCTRL*, control siRNA; *siC2*, caspase-2 siRNA. Scale bars represent 1000 μm.

to decrease palmitate-induced reactive oxygen species and ceramide generation (45, 46). To determine whether the cell death induced by palmitate in 293T cells was mediated by either of these two stresses, we treated cells with the reactive oxygen species scavenger *N*-acetylcysteine or the serine palmitoyltransferase inhibitor myriocin to inhibit ceramide synthesis. Neither treatment was able to suppress cell death induced by palmitate, suggesting that palmitate-induced apoptosis is not dependent on reactive oxygen species or ceramide formation in these cells (data not shown). Thus, to more thoroughly understand how palmitate exerts its proapoptotic effects on caspase-2, we tested whether metabolism of palmitate to its corresponding long-chain acyl-CoA and/or long-chain acylcarnitine form was required to induce caspase-2 activity and cell death. Activation of other caspases, specifically caspase-3, -7, and -8, has been shown to be directly induced by palmitoylcarnitine *in vitro* (47), and therefore, it seemed possible that caspase-2 was being activated by palmitate via its conversion to palmitoylcarnitine. To explore this possibility, we treated cells with the long-chain acyl-CoA synthetase inhibitor triacsin C and the carnitine palmitoyltransferase I inhibitor etomoxir and assessed caspase-2 activity following palmitate treatment. Triacsin C, which inhibits the formation of palmitoyl-CoA, significantly prevented palmitate-induced caspase-2 activation, whereas etomoxir, which inhibits the formation of palmitoylcarnitine, had no significant effect (Fig. 6*B*). Consistent with caspase-2 being the initiator of apoptosis in this setting, triacsin C was also able to inhibit cell death, whereas etomoxir failed to show any effect (Fig. 6*C*). Together, these data suggest that although palmitate activation via acyl-CoA formation was essential to induce caspase-2 activation palmitoylcarnitine formation was not required. It is important to note that in our experimental setting triacsin C revealed cytotoxic effects in the absence of palmitate, which may be due to a reduction of basal intracellular acyl-CoA concentrations below a level necessary for cell viability (data not shown).

Caspase-2 Is Required for LCFA-induced Apoptosis in Hepatocytes—To more thoroughly evaluate the importance of caspase-2 in lipoapoptosis, we examined the role of caspase-2 in saturated LCFA-induced hepatocyte cell death. Accumulating evidence suggests that lipoapoptosis plays an important role in the pathogenesis of nonalcoholic fatty liver disease (NAFLD) as well as in the progression from NAFLD to the more advanced state of liver disease, nonalcoholic steatohepatitis (6, 48). Hepatocyte apoptosis is significantly increased in patients with nonalcoholic steatohepatitis and has been shown to enhance liver fibrogenesis and the development of cirrhosis, both of which correlate with negative patient outcomes (49, 50). There are currently no effective therapies that halt NAFLD progression, and thus, insight into the molecular mediators of lipoapoptosis may be useful in developing effective therapies for this syndrome (6).

To determine whether caspase-2 is required for lipoapoptosis in hepatocytes, we tested whether knockdown of caspase-2 in HepG2 cells would protect against palmitate-induced cell death. As shown in Fig. 6*A*, down-regulation of caspase-2 was

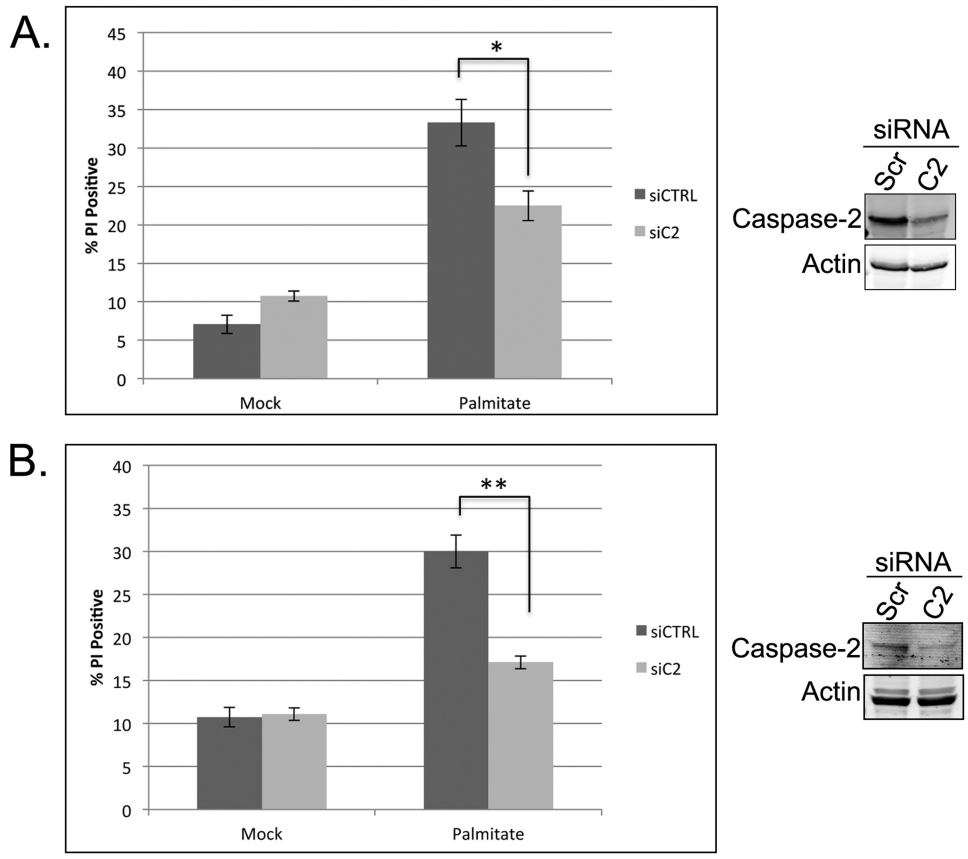

FIGURE 7. **Caspase-2 is required for LCFA-induced apoptosis in hepatocytes.** *A*, HepG2 cells were transfected with 50 nM scrambled or caspase-2 (*C2*)-targeted siRNA. At 48 h post-transfection, cells were mock-treated with BSA or treated with 0.7 mM palmitate for 24 h, and cell death was measured by propidium iodide (*PI*) staining and flow cytometric analysis. Knockdown efficiency was determined by immunoblot. *B*, AML12 cells were treated with 50 nM scrambled (*Scr*) or mouse caspase-2-targeted SMARTpool siRNA. At 48 h post-transfection, cells were mock- or palmitate-treated and analyzed for cell death as in *A*. Knockdown efficiency was determined by immunoblot. The results represent the means ± S.E. (*error bars*) for three or more independent experiments. Statistical significance was determined using a two-tailed Student's *t* test. *, $p < 0.05$ *versus* control; **, $p < 0.01$ *versus* control. *siCTRL*, control siRNA; *siC2*, caspase-2 siRNA.

able to dampen cell death as determined by propidium iodide staining. Although the decrease in cell death is clear upon caspase-2 knockdown, it is not complete. The lack of a larger effect may be due to residual caspase-2 as we were only able to achieve partial knockdown in this cell type (Fig. 7*A*). Therefore, we also investigated whether caspase-2 was activated in normal mouse hepatocytes (AML12 cells) following palmitate treatment by measuring VDVAD-*p*NA cleavage. We observed a 45% increase in enzymatic activity, consistent with a role for caspase-2 in palmitate-induced cell death in hepatocytes (data not shown). To determine whether caspase-2 was required for cell death, we pretreated AML12 cells with scrambled or caspase-2 siRNA and assessed cell death after palmitate treatment. Down-regulation of caspase-2 significantly inhibited cell death in these normal mouse hepatocytes (Fig. 7*B*), revealing a conserved, critical role for caspase-2 in saturated LCFA-induced cell death.

DISCUSSION

With the prevalence of obesity and metabolic syndrome rising sharply worldwide, it has become increasingly important to define the molecular mechanisms underlying the pathogenesis and progression of diseases associated with these disorders. Lipoapoptosis has recently gained recognition as a critical mediator of diseases associated with metabolic syndrome, including type 2 diabetes mellitus, cardiovascular disease, and NAFLD (3, 5, 6). In this report, we demonstrate a novel role for caspase-2 as an initiator of lipoapoptosis. Using a metabolomics approach, we discovered that the activation of caspase-2, the initiator of apoptosis in *Xenopus* egg extracts, is associated with an accumulation of LCFAs. Metabolic treatments that blocked the buildup of LCFAs also potently inhibited caspase-2 activation. Together, these observations led us to investigate whether caspase-2 is engaged and activated in mammalian cells in response to LCFA treatment. We demonstrated that caspase-2 is not only engaged but makes a significant contribution to saturated LCFA-induced cell death both in 293T cells and several hepatocyte cell lines. Together, these findings reveal a previously unknown role for caspase-2 as an initiator caspase and provide a missing link in the signaling pathways functioning upstream of the mitochondria in lipoapoptosis.

Metabolomic profiling of *Xenopus* egg extract revealed a clear metabolic signature that emerged upon extract incubation. Several metabolic changes were observed prior to caspase activation, including a decrease in aspartate, an increase in alanine, an accumulation of succinate, and a buildup of multiple long-chain acylcarnitines, which reflect the cognate acyl-CoA

pools. Although the utilization of amino acids as a carbon source was not surprising as this had been observed previously in *Xenopus* eggs (24), the buildup of succinate and LCFA metabolites was not anticipated. Because the metabolic profile of incubated extract showed striking similarity to previous studies of hypoxic systems, we measured mitochondrial oxygen consumption and discovered that extracts fail to consume oxygen during the assessed room temperature incubation period. Based on previous findings and the lack of oxygen consumption in this system, we speculate that the observed metabolic changes are the result of inhibited electron transport chain activity, which would result in an insufficient supply of oxidized electron carriers (*i.e.* NAD^+). As a result, succinate dehydrogenase, the only enzyme that participates in both the electron transport chain and the TCA cycle, would be unable to efficiently oxidize succinate, leading to its accumulation and a decrease in TCA cycle flux. A block in succinate metabolism would lead to a decrease in anaplerotic substrates, mainly oxaloacetate, resulting in the accumulation of acetyl-CoA (C2) and pyruvate, as we have observed. Furthermore, inefficient flux of substrates through the TCA cycle without the ability to efficiently regenerate NAD^+ would likely lead to a redox imbalance, resulting in increased levels of NADH. To compensate for these accumulations, pyruvate would be converted to lactate in a process that regenerates NAD^+. The large increase in lactate that occurs upon extract incubation is likely driven by NADH accumulation. Furthermore, we speculate that the buildup of LCFA metabolites is also linked to increasing NADH levels, which in combination with high levels of acetyl-CoA can feed back and inhibit β-oxidation.

Using an inhibitor of aminotransferases, we demonstrated that blocking the use of aspartate as a carbon source could delay caspase-2 activation in aging extracts. This effect did not appear to be due to amino acid stabilization but rather appeared to be the result of a decrease in LCFA accumulation. The ability of AOA to suppress buildup of LCFA metabolites is likely mediated by its ability to block carbon flux through the TCA cycle, which helps to stabilize early changes in NAD^+/NADH (*i.e.* slowing the decrease we observed in untreated extracts; Fig. 3*D*), allowing continued β-oxidation. AOA treatment was unable to restore mitochondrial respiration (data not shown), making it more likely that AOA is delaying NADH accumulation rather than accelerating NAD^+ regeneration. Palmitate treatment can likely override the suppressive effect of AOA by accelerating lipid overload. The ability of palmitate to both accelerate caspase activation and override the suppressive effect of AOA suggests that an excess of saturated LCFAs can trigger the activation of caspase-2.

Although the *Xenopus* egg extract metabolomics may not reflect the metabolic state of unstressed mammalian cells, the observed metabolic signature was very reminiscent of several pathophysiological disease states. For example, succinate and LCFA accumulations have been observed in hypoxia, diabetes, and cancer and have been attributed to an imbalance between energy demand and food/oxygen supply (51–53). Although the underlying cause of such an imbalance remains uncertain in the extract, we hypothesized that the critical metabolic stress triggering caspase-2 activation and apoptosis was the accumulation of LCFAs. Lipid-induced cytotoxicity plays an important role in the etiology of multiple metabolic disorders, including heart disease, type 2 diabetes mellitus, and NAFLD, and as such, we were interested in determining whether caspase-2 might be mediating lipoapoptosis in mammalian somatic cells.

Our data suggest that caspase-2 is activated following palmitate treatment as shown by both cleavage of the preferred caspase-2 substrate, VDVAD, and proteolytic processing of the caspase-2 proenzyme. Furthermore, we demonstrated that caspase-2 was activated by recruitment to a high molecular weight complex following palmitate treatment and that caspase-2 was required for full activation of palmitate-induced cell death. Delving further into caspase-2-induced lipotoxicity, we demonstrated that only saturated fatty acids induced cell death and that this cell death was dependent on caspase-2. Interestingly, as has been observed previously in other cells types, palmitate-induced cytotoxicity was not dependent on reactive oxygen species, ceramides, or oxidative LCFA catabolism in 293T cells (37–39). Rather, the activation of palmitate via acyl-CoA formation was required to induce cell death. Understanding how saturated LCFAs and their respective acyl-CoA derivatives induce caspase-2 activation will be the focus of future studies.

Finally, we show that caspase-2 functions as the initiator of cell death in saturated LCFA-induced hepatocyte cell death. This hepatocyte finding is of particular interest as lipoapoptosis plays a critical role in the development and progression of NAFLD, the most common form of chronic liver disease in both children and adults in the United States (54, 55). Because apoptosis plays such an important role in NAFLD progression, inhibition of apoptosis has been proposed as a useful therapeutic strategy. In support of this idea, recent studies performed in both humans and mice have shown moderate success of pan-caspase inhibitors on NAFLD symptoms (56, 57). Our data suggest that an inhibitor that more specifically targets caspase-2 may enhance the effectiveness of caspase-targeted therapies. Finally, although our studies have focused on the importance of caspase-2 in hepatocyte lipoapoptosis, there are several additional settings where caspase-2 may be relevant in lipoapoptotic therapies, including cardiomyocytes in the heart, proximal tubule cells in the kidney, and islet beta cells in the pancreas. The loss of this apical initiator caspase does not appear to compromise viability in a knock-out setting, and thus, caspase-2 is an attractive therapeutic target for both blocking apoptosis and maintaining mitochondrial integrity in disease states. Future studies will evaluate the physiological relevance of caspase-2 in these lipotoxicity settings.

Acknowledgments—We thank Kenkyo Matsuura, Chih-Cheng Yang, and Bofu Huang as well as the rest of the Kornbluth laboratory for helpful discussion.

REFERENCES

1. Frayn, K. N. (2002) Adipose tissue as a buffer for daily lipid flux. *Diabetologia* **45,** 1201–1210
2. Lewis, G. F., Carpentier, A., Adeli, K., and Giacca, A. (2002) Disordered fat storage and mobilization in the pathogenesis of insulin resistance and type 2 diabetes. *Endocr. Rev.* **23,** 201–229

3. Kusminski, C. M., Shetty, S., Orci, L., Unger, R. H., and Scherer, P. E. (2009) Diabetes and apoptosis: lipotoxicity. *Apoptosis* **14,** 1484–1495
4. Unger, R. H., Clark, G. O., Scherer, P. E., and Orci, L. (2010) Lipid homeostasis, lipotoxicity and the metabolic syndrome. *Biochim. Biophys. Acta* **1801,** 209–214
5. Listenberger, L. L., and Schaffer, J. E. (2002) Mechanisms of lipoapoptosis: implications for human heart disease. *Trends Cardiovasc. Med.* **12,** 134–138
6. Cazanave, S. C., and Gores, G. J. (2010) Mechanisms and clinical implications of hepatocyte lipoapoptosis. *Clin. Lipidol.* **5,** 71–85
7. Malhi, H., Bronk, S. F., Werneburg, N. W., and Gores, G. J. (2006) Free fatty acids induce JNK-dependent hepatocyte lipoapoptosis. *J. Biol. Chem.* **281,** 12093–12101
8. de Vries, J. E., Vork, M. M., Roemen, T. H., de Jong, Y. F., Cleutjens, J. P., van der Vusse, G. J., and van Bilsen, M. (1997) Saturated but not mono-unsaturated fatty acids induce apoptotic cell death in neonatal rat ventricular myocytes. *J. Lipid Res.* **38,** 1384–1394
9. Arici, M., Chana, R., Lewington, A., Brown, J., and Brunskill, N. J. (2003) Stimulation of proximal tubular cell apoptosis by albumin-bound fatty acids mediated by peroxisome proliferator activated receptor-γ. *J. Am. Soc. Nephrol.* **14,** 17–27
10. El-Assaad, W., Buteau, J., Peyot, M. L., Nolan, C., Roduit, R., Hardy, S., Joly, E., Dbaibo, G., Rosenberg, L., and Prentki, M. (2003) Saturated fatty acids synergize with elevated glucose to cause pancreatic β-cell death. *Endocrinology* **144,** 4154–4163
11. Unger, R. H., and Orci, L. (2002) Lipoapoptosis: its mechanism and its diseases. *Biochim. Biophys. Acta* **1585,** 202–212
12. Danial, N. N., and Korsmeyer, S. J. (2004) Cell death: critical control points. *Cell* **116,** 205–219
13. Kluck, R. M., Martin, S. J., Hoffman, B. M., Zhou, J. S., Green, D. R., and Newmeyer, D. D. (1997) Cytochrome c activation of CPP32-like proteolysis plays a critical role in a *Xenopus* cell-free apoptosis system. *EMBO J.* **16,** 4639–4649
14. Liu, X., Kim, C. N., Yang, J., Jemmerson, R., and Wang, X. (1996) Induction of apoptotic program in cell-free extracts: requirement for dATP and cytochrome c. *Cell* **86,** 147–157
15. Tu, S., McStay, G. P., Boucher, L.-M., Mak, T., Beere, H. M., and Green, D. R. (2006) *In situ* trapping of activated initiator caspases reveals a role for caspase-2 in heat shock-induced apoptosis. *Nat. Cell Biol.* **8,** 72–77
16. Ho, L. H., Read, S. H., Dorstyn, L., Lambrusco, L., and Kumar, S. (2008) Caspase-2 is required for cell death induced by cytoskeletal disruption. *Oncogene* **27,** 3393–3404
17. Imre, G., Heering, J., Takeda, A. N., Husmann, M., Thiede, B., zu Heringdorf, D. M., Green, D. R., van der Goot, F. G., Sinha, B., Dötsch, V., and Rajalingam, K. (2012) Caspase-2 is an initiator caspase responsible for pore-forming toxin-mediated apoptosis. *EMBO J.* **31,** 2615–2628
18. Bonzon, C., Bouchier-Hayes, L., Pagliari, L. J., Green, D. R., and Newmeyer, D. D. (2006) Caspase-2-induced apoptosis requires bid cleavage: a physiological role for bid in heat shock-induced death. *Mol. Biol. Cell* **17,** 2150–2157
19. Li, H., Zhu, H., Xu, C. J., and Yuan, J. (1998) Cleavage of BID by caspase 8 mediates the mitochondrial damage in the Fas pathway of apoptosis. *Cell* **94,** 491–501
20. Bergeron, L., Perez, G. I., Macdonald, G., Shi, L., Sun, Y., Jurisicova, A., Varmuza, S., Latham, K. E., Flaws, J. A., Salter, J. C., Hara, H., Moskowitz, M. A., Li, E., Greenberg, A., Tilly, J. L., and Yuan, J. (1998) Defects in regulation of apoptosis in caspase-2-deficient mice. *Genes Dev.* **12,** 1304–1314
21. Nutt, L. K., Margolis, S. S., Jensen, M., Herman, C. E., Dunphy, W. G., Rathmell, J. C., and Kornbluth, S. (2005) Metabolic regulation of oocyte cell death through the CaMKII-mediated phosphorylation of caspase-2. *Cell* **123,** 89–103
22. Andersen, J. L., Thompson, J. W., Lindblom, K. R., Johnson, E. S., Yang, C. S., Lilley, L. R., Freel, C. D., Moseley, M. A., and Kornbluth, S. (2011) A biotin switch-based proteomics approach identifies 14-3-3ζ as a target of Sirt1 in the metabolic regulation of caspase-2. *Mol. Cell* **43,** 834–842
23. Nutt, L. K., Buchakjian, M. R., Gan, E., Darbandi, R., Yoon, S. Y., Wu, J. Q., Miyamoto, Y. J., Gibbons, J. A., Andersen, J. L., Freel, C. D., Tang, W., He, C., Kurokawa, M., Wang, Y., Margolis, S. S., Fissore, R. A., and Kornbluth, S. (2009) Metabolic control of oocyte apoptosis mediated by 14-3-3ζ-regulated dephosphorylation of caspase-2. *Dev. Cell* **16,** 856–866
24. Dworkin, M. B., and Dworkin-Rastl, E. (1990) Regulation of carbon flux from amino acids into sugar phosphates in *Xenopus* embryos. *Dev. Biol.* **138,** 177–187
25. Dworkin, M. B., and Dworkin-Rastl, E. (1991) Carbon metabolism in early amphibian embryos. *Trends Biochem. Sci.* **16,** 229–234
26. Smythe, C., and Newport, J. W. (1991) Systems for the study of nuclear assembly, DNA replication, and nuclear breakdown in *Xenopus laevis* egg extracts. *Methods Cell Biol.* **35,** 449–468
27. An, J., Muoio, D. M., Shiota, M., Fujimoto, Y., Cline, G. W., Shulman, G. I., Koves, T. R., Stevens, R., Millington, D., and Newgard, C. B. (2004) Hepatic expression of malonyl-CoA decarboxylase reverses muscle, liver and whole-animal insulin resistance. *Nat. Med.* **10,** 268–274
28. Shiokawa, K., Tashiro, K., Atsuchi, Y., and Kawazoe, Y. (1986) Alteration of the pool of free amino acids during oogenesis, oocyte maturation and embryogenesis of *Xenopus laevis* and *Xenopus borealis*. *Zool. Sci.* **3,** 793–799
29. Vastag, L., Jorgensen, P., Peshkin, L., Wei, R., Rabinowitz, J. D., and Kirschner, M. W. (2011) Remodeling of the metabolome during early frog development. *PLoS One* **6,** e16881
30. Folbergrová, J., Ljunggren, B., Norberg, K., and Siesjö, B. K. (1974) Influence of complete ischemia on glycolytic metabolites, citric acid cycle intermediates, and associated amino acids in the rat cerebral cortex. *Brain Res.* **80,** 265–279
31. Wiesner, R. J., Deussen, A., Borst, M., Schrader, J., and Grieshaber, M. K. (1989) Glutamate degradation in the ischemic dog heart: contribution to anaerobic energy production. *J. Mol. Cell. Cardiol.* **21,** 49–59
32. Kotarsky, H., Keller, M., Davoudi, M., Levéen, P., Karikoski, R., Enot, D. P., and Fellman, V. (2012) Metabolite profiles reveal energy failure and impaired β-oxidation in liver of mice with complex III deficiency due to a BCS1L mutation. *PLoS One* **7,** e41156
33. Hochachka, P. W., Owen, T. G., Allen, J. F., and Whittow, G. C. (1975) Multiple end products of anaerobiosis in diving vertebrates. *Comp. Biochem. Physiol. B* **50,** 17–22
34. Taegtmeyer, H. (1978) Metabolic responses to cardiac hypoxia. Increased production of succinate by rabbit papillary muscles. *Circ. Res.* **43,** 808–815
35. Lupi, R., Dotta, F., Marselli, L., Del Guerra, S., Masini, M., Santangelo, C., Patané, G., Boggi, U., Piro, S., Anello, M., Bergamini, E., Mosca, F., Di Mario, U., Del Prato, S., and Marchetti, P. (2002) Prolonged exposure to free fatty acids has cytostatic and pro-apoptotic effects on human pancreatic islets: evidence that β-cell death is caspase mediated, partially dependent on ceramide pathway, and Bcl-2 regulated. *Diabetes* **51,** 1437–1442
36. Fürstova, V., Kopska, T., James, R. F., and Kovar, J. (2008) Comparison of the effect of individual saturated and unsaturated fatty acids on cell growth and death induction in the human pancreatic β-cell line NES2Y. *Life Sci.* **82,** 684–691
37. Hardy, S., El-Assaad, W., Przybytkowski, E., Joly, E., Prentki, M., and Langelier, Y. (2003) Saturated fatty acid-induced apoptosis in MDA-MB-231 breast cancer cells: a role for cardiolipin. *J. Biol. Chem.* **278,** 31861–31870
38. Staiger, K., Staiger, H., Weigert, C., Haas, C., Häring, H.-U., and Kellerer, M. (2006) Saturated, but not unsaturated, fatty acids induce apoptosis of human coronary artery endothelial cells via nuclear factor-κB activation. *Diabetes* **55,** 3121–3126
39. Kim, J. E., Ahn, M. W., Baek, S. H., Lee, I. K., Kim, Y. W., Kim, J. Y., Dan, J. M., and Park, S. Y. (2008) AMPK activator, AICAR, inhibits palmitate-induced apoptosis in osteoblast. *Bone* **43,** 394–404
40. Mei, S., Ni, H. M., Manley, S., Bockus, A., Kassel, K. M., Luyendyk, J. P., Copple, B. L., and Ding, W. X. (2011) Differential roles of unsaturated and saturated fatty acids on autophagy and apoptosis in hepatocytes. *J. Pharmacol. Exp. Ther.* **339,** 487–498
41. Listenberger, L. L., Han, X., Lewis, S. E., Cases, S., Farese, R. V., Jr., Ory, D. S., and Schaffer, J. E. (2003) Triglyceride accumulation protects against fatty acid-induced lipotoxicity. *Proc. Natl. Acad. Sci. U.S.A.* **100,** 3077–3082
42. Miller, T. A., LeBrasseur, N. K., Cote, G. M., Trucillo, M. P., Pimentel,

D. R., Ido, Y., Ruderman, N. B., and Sawyer, D. B. (2005) Oleate prevents palmitate-induced cytotoxic stress in cardiac myocytes. *Biochem. Biophys. Res. Commun.* **336,** 309–315
43. Coll, T., Eyre, E., Rodríguez-Calvo, R., Palomer, X., Sánchez, R. M., Merlos, M., Laguna, J. C., and Vázquez-Carrera, M. (2008) Oleate reverses palmitate-induced insulin resistance and inflammation in skeletal muscle cells. *J. Biol. Chem.* **283,** 11107–11116
44. Gao, D., Griffiths, H. R., and Bailey, C. J. (2009) Oleate protects against palmitate-induced insulin resistance in L6 myotubes. *Br. J. Nutr.* **102,** 1557–1563
45. Yuzefovych, L., Wilson, G., and Rachek, L. (2010) Different effects of oleate vs. palmitate on mitochondrial function, apoptosis, and insulin signaling in L6 skeletal muscle cells: role of oxidative stress. *Am. J. Physiol. Endocrinol. Metab.* **299,** E1096–E1105
46. Hu, W., Ross, J., Geng, T., Brice, S. E., and Cowart, L. A. (2011) Differential regulation of dihydroceramide desaturase by palmitate *versus* monounsaturated fatty acids: implications for insulin resistance. *J. Biol. Chem.* **286,** 16596–16605
47. Mutomba, M. C., Yuan, H., Konyavko, M., Adachi, S., Yokoyama, C. B., Esser, V., McGarry, J. D., Babior, B. M., and Gottlieb, R. A. (2000) Regulation of the activity of caspases by L-carnitine and palmitoylcarnitine. *FEBS Lett.* **478,** 19–25
48. Ibrahim, S. H., Kohli, R., and Gores, G. J. (2011) Mechanisms of lipotoxicity in NAFLD and clinical implications. *J. Pediatr. Gastroenterol. Nutr.* **53,** 131–140
49. Canbay, A., Higuchi, H., Bronk, S. F., Taniai, M., Sebo, T. J., and Gores, G. J. (2002) Fas enhances fibrogenesis in the bile duct ligated mouse: a link between apoptosis and fibrosis. *Gastroenterology* **123,** 1323–1330
50. Feldstein, A. E., Canbay, A., Angulo, P., Taniai, M., Burgart, L. J., Lindor, K. D., and Gores, G. J. (2003) Hepatocyte apoptosis and Fas expression are prominent features of human nonalcoholic steatohepatitis. *Gastroenterology* **125,** 437–443
51. Goldberg, N. D., Passonneau, J. V., and Lowry, O. H. (1966) Effects of changes in brain metabolism on the levels of citric acid cycle intermediates. *J. Biol. Chem.* **241,** 3997–4003
52. Sadagopan, N., Li, W., Roberds, S. L., Major, T., Preston, G. M., Yu, Y., and Tones, M. A. (2007) Circulating succinate is elevated in rodent models of hypertension and metabolic disease. *Am. J. Hypertens.* **20,** 1209–1215
53. Selak, M. A., Armour, S. M., MacKenzie, E. D., Boulahbel, H., Watson, D. G., Mansfield, K. D., Pan, Y., Simon, M. C., Thompson, C. B., and Gottlieb, E. (2005) Succinate links TCA cycle dysfunction to oncogenesis by inhibiting HIF-α prolyl hydroxylase. *Cancer Cell* **7,** 77–85
54. Wieckowska, A., and Feldstein, A. E. (2005) Nonalcoholic fatty liver disease in the pediatric population: a review. *Curr. Opin. Pediatr.* **17,** 636–641
55. Browning, J. D., Szczepaniak, L. S., Dobbins, R., Nuremberg, P., Horton, J. D., Cohen, J. C., Grundy, S. M., and Hobbs, H. H. (2004) Prevalence of hepatic steatosis in an urban population in the United States: impact of ethnicity. *Hepatology* **40,** 1387–1395
56. Ratziu, V., Sheikh, M. Y., Sanyal, A. J., Lim, J. K., Conjeevaram, H., Chalasani, N., Abdelmalek, M., Bakken, A., Renou, C., Palmer, M., Levine, R. A., Bhandari, B. R., Cornpropst, M., Liang, W., King, B., Mondou, E., Rousseau, F. S., McHutchison, J., and Chojkier, M. (2012) A phase 2, randomized, double-blind, placebo-controlled study of GS-9450 in subjects with nonalcoholic steatohepatitis. *Hepatology* **55,** 419–428
57. Witek, R. P., Stone, W. C., Karaca, F. G., Syn, W. K., Pereira, T. A., Agboola, K. M., Omenetti, A., Jung, Y., Teaberry, V., Choi, S. S., Guy, C. D., Pollard, J., Charlton, P., and Diehl, A. M. (2009) Pan-caspase inhibitor VX-166 reduces fibrosis in an animal model of nonalcoholic steatohepatitis. *Hepatology* **50,** 1421–1430